Spontaneous Vesiculation of Aqueous Lipid Dispersions

H. Hauser,*,‡ N. Gains,‡ H.-J. Eibl,§ M. Müller,∥ and E. Wehrli∥

Laboratorium für Biochemie and Laboratorium für Elektronenmikroskopie I, Institut für Zellbiologie, Eidgenössiche Technische Hochschule Zürich, CH 8092 Zürich, Switzerland, and Max-Planck-Institut für biophysikalische Chemie, D 3400 Göttingen, Federal Republic of Germany

Received July 9, 1985

ABSTRACT: The swelling properties of lipid mixtures consisting of phosphatidylcholine and a charged single-chain detergent have been studied. The work presented here is confined to lipid mixtures forming smectic lamellar phases in H_2O. These mixtures exhibit continuous swelling with increasing water content, provided the surface charge density exceeds a threshold value of about 1–2 $\mu C/cm^2$. In excess H_2O, such mixtures undergo spontaneous vesiculation: unilamellar vesicles form spontaneously when excess H_2O or salt solutions of moderate ionic strength ($I < 0.2$) are added to the dried film of such lipid mixtures. The resulting dispersion of unilamellar vesicles is usually polydisperse. Its average size depends on the detergent/phospholipid mole ratio, decreasing with increasing detergent content. It is shown that in the phase diagram of three-component systems consisting of phosphatidylcholine, a charged single-chain detergent, and excess H_2O there is a compositional range, though narrow, within which the small unilamellar vesicle (diameter < 100 nm) is the thermodynamically most stable structure. This behavior is characteristic of charged, single-chain detergents of 14 and more C atoms. Many pharmacologically active compounds are amphiphilic and surface-active, and as such, they will orient at phospholipid–water interfaces, imparting a net surface charge to neutral lipid surfaces. It is shown that such drugs exhibit detergent-like action. Mixed films of phosphatidylcholine and a pharmacologically active compound behave similarly to phosphatidylcholine–detergent mixtures: they undergo spontaneous vesiculation when excess H_2O or salt solutions of moderate ionic strength are added. In this case, the drug itself induces vesiculation; possible pharmacological implications of this finding are discussed.

Phospholipid bilayers are now generally accepted to be an integral part of biological membranes. Both multilamellar and unilamellar phospholipid vesicles have been widely used as model membranes to study (I) the intrinsic bilayer properties, (II) the interaction of phospholipid bilayers with ions and proteins, and (III) membrane-mediated processes. This last application, for which the term membrane mimetic chemistry has been coined, is becoming increasingly important. It involves processes such as membrane fusion, the control of reaction rates at interfaces, solar energy conversion, and drug delivery. In this field of application simple, quick, and inexpensive methods for the preparation of lipid bilayer systems are required. Furthermore, the methodology must be versatile, allowing the production of bilayer vesicles differing widely in size, chemical and physical stability, and bilayer properties, e.g., surface charge density, bilayer fluidity, and permeability. Lipid technology has advanced considerably in the last decade, and in its present state, it should be possible to meet even very specific requirements. Previously, we described a simple and quick method for producing unilamellar vesicles (Hauser & Gains, 1982). Spontaneous vesiculation was induced in aqueous dispersions of phosphatidic acid (PA) and mixtures of this phospholipid with phosphatidylcholines (PC) by a transient increase in pH effecting the full ionization of the phosphate group of PA. The resulting phospholipid dispersion was shown to consist of small unilamellar vesicles (SUV)[1] of a narrow particle size distribution and large unilamellar vesicles (LUV) of a heterogeneous size distribution (Hauser et al., 1983; Gains & Hauser, 1983, 1984; Schurtenberger & Hauser, 1984). Here, we show that spontaneous vesiculation is a general phenomenon occurring much more widely than previously anticipated. Lipid mixtures of a particular composition consisting of isoelectric phosphatidylcholine and a charged amphiphile undergo spontaneous vesiculation when dispersed in excess H_2O or aqueous media of moderate ionic strength ($I < 0.2$).

Materials and Methods

Egg phosphatidylcholine (EPC) was purchased from Lipid Products (Surrey, U.K.), ox brain lysophosphatidylserine from Avanti Polar Lipid (Birmingham, AL), and lysophosphatidylglycerol, cetyltrimethylammonium bromide (CTAB), tetradecyltrimethylammonium bromide (TTAB), and dodecyltrimethylammonium bromide (DTAB) from Sigma. Dimyristoyl-PC was obtained from R. Berchtold (Biochemisches Laboratorium, Bern, Switzerland). Chlorpromazine and gramicidin S dihydrochloride were purchased from Sigma, St. Louis, MO. The C, H, and N microanalysis of these two compounds was consistent with their chemical formulas. The phospholipids were pure by TLC standard. The purity of the phospholipids, detergents, and chlorpromazine was checked by ^1H NMR and found to be at least 99%.

Essentially two groups of phosphate-containing amphiphiles were synthesized: (1) the first group is of the general structure

‡ Laboratorium für Biochemie, Eidgenössiche Technische Hochschule Zürich.

§ Max-Planck-Institut für biophysikalische Chemie.

∥ Laboratorium für Elektronenmikroskopie I, Eidgenössische Technische Hochschule Zürich.

[1] Abbreviations: EPC, egg phosphatidylcholine; SUV, small unilamellar vesicles; LUV, large unilamellar vesicles; HDMPP, sodium salt of 3-hexadecanoyl-2,2-dimethylpropanediol 1-phosphate; CTAB, cetyltrimethylammonium bromide; TTAB, tetradecyltrimethylammonium bromide; DTAB, dodecyltrimethylammonium bromide; lyso-PG, lysophosphatidylglycerol; lyso-PS, lysophosphatidylserine; CPC, cetylpyridinium chloride; TLC, thin-layer chromatography; ESR, electron spin resonance.

0006-2960/86/0425-2126$01.50/0

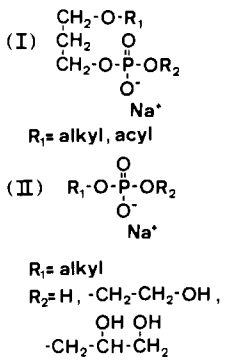

FIGURE 1: Chemical formulas of phosphate-containing detergents.

I (Figure 1) with the propanediol 1-phosphate group being the central part of the molecule and where R_1 is a long-chain alkyl or acyl group with 16 or 18 carbon atoms and R_2 is either a proton, β-hydroxyethyl, β-bromoethyl, or 2,3-dihydroxypropyl. The second group is of the general structure II (Figure 1), where R_1 is alkyl with 14–20 carbon atoms and R_2 is as described above. The synthesis of these two groups of phosphate-containing detergents was carried out as described before (Eibl, 1980).

Preparation of Lipid Dispersion. It should be stressed at the outset that all phospholipid dispersions were made without sonication unless stated otherwise. Mixed dispersions consisting of EPC and various amphiphiles in H_2O were prepared as follows: a solution of 10–20 mg of EPC and the amphiphile in 1 mL of $CHCl_3/CH_3OH$ (2:1 v/v) was dried down in a round-bottomed flask by rotary evaporation at room temperature, and the film was thoroughly dried under vacuum. With amphiphiles containing a secondary phosphate group (i.e., a phosphodiester group), 1 mL of H_2O, or D_2O for NMR measurement, was added, and the lipid mixture was dispersed by vortex mixing for 5 min. The pH of the dispersion was brought to ~8.5 by adding NaOH, or NaOD for NMR experiments. With amphiphiles containing a primary phosphate group, sufficient NaOH or NaOD was added to the dry film to bring the apparent pH to 11–12. After the addition of sodium hydroxide, the pH was immediately reduced to neutrality by adding HCl or DCl. Lipid mixtures containing EPC and a positively charged amphiphile (detergent or pharmacologically active compound) were dispersed by adding 1 ml of H_2O or D_2O (for NMR) at neutral pH to the dried film made of EPC and amphiphile and vortex mixing as described above.

NMR Measurements. ^1H NMR spectra were recorded at 90 and 360 MHz on Bruker Fourier-transform spectrometers. Spectral intensities were measured by integration with CH_3-COONa as an internal integration standard. In order to avoid saturation of the acetate standard, a relaxation delay of ~20 s was used before each pulse. The error of the intensity measurement was usually within about 10–30%; it increased with decreasing signal intensity. The hydrocarbon chain signal, hitherto referred to as CH_2 signal, is here defined as the sum of all ^1H resonances upfield of the CH_3COONa standard. Its intensity was measured as the total integral upfield of the CH_3COONa standard (Hauser et al., 1983). The apparent pH of the NMR samples was measured in 5-mm NMR tubes with a combined glass electrode of a diameter of ~3 mm. If necessary, the apparent pH was adjusted by adding small volumes of NaOD or DCl solutions.

Filtration through Nucleopore Filters. Lipid dispersions (0.5 mL, 1–10 mg/mL) were filtered through nucleopore polycarbonate capillary pore filters (Pleasanton, CA) in a 3-mL Amicon filtration cell under a pressure of up to ~1 atm (~10^5 N m^{-2}). The filter was rinsed with an excess of ~5 mL of 0.05 M NaCl, and the lipid content in the filtrate was determined by phosphate analysis (Gains & Hauser, 1984). Some filtration experiments gave erratic results, which were discarded. The reason for this is probably the clogging of the filter pores with lipid particles of a diameter approximating that of the filter pores.

Separation of Large Multilamellar Liposomes from Unilamellar Vesicles. Lipid dispersions in H_2O were centrifuged at 20000*g* for 5 min. This treatment was shown to remove quantitatively multilamellar structures (Gains & Hauser, 1983). The phospholipid in the supernatant was determined as phosphate (Gains & Hauser, 1984). The turbidity of the lipid dispersions was monitored by measuring absorbance at 340 nm.

Other Methods. Electron microscopy (Müller et al., 1980; Hauser et al., 1983) and ESR spin-labeling experiments (Hauser et al., 1982) were carried out as described previously. For the ESR experiments, 5-doxylstearate (from Molecular Probes, Junction City, OR) was incorporated in the lipid dispersion at a lipid/spin-label mole ratio of 200:1, and ESR order parameters were measured as described before (Hauser et al., 1982).

RESULTS

Spontaneous Vesiculation of Lipid Mixtures Containing Negatively or Positively Charged Detergents. Mixed dispersions of HDMPP and EPC in H_2O were prepared as described under Materials and Methods, and the effect of increasing quantities of the detergent HDMPP incorporated in EPC bilayers on the ^1H NMR spectra of these dispersions is shown in Figure 2. As the amphiphile content of the bilayer was increased, a ^1H high-resolution spectrum developed with line widths characteristic of SUV. Figure 3A shows how the ^1H signal intensity of the two prominent EPC resonances at 1.28 ppm (CH_2 signal) and at 3.25 ppm [$-N(CH_3)_3$] increased with increasing HDMPP content. At an amphiphile content of ~50%, 50–70% of the total lipid (=sum of amphiphile and phospholipid) contributed to the ^1H high-resolution spectrum. At even higher amphiphile concentrations, all the lipid contributed to the ^1H NMR spectrum. Under these conditions some resonances show spin–spin hyperfine interactions indicative of the presence of small micelles. Also shown in Figure 3A is the amount of phospholipid (%) that is recovered in the filtrate after filtering the lipid dispersion through a nucleopore filter with a nominal pore diameter of 80 nm (shaded area). Between ~30 and 40% amphiphile there was a steep increase in the lipid material passing through the filter. This increase is reasonably well correlated with the ^1H signal intensities.

Ten other phosphate-containing amphiphiles of the general structure I or II (Figure 1) were tested as to their dispersing effect on EPC bilayers. Qualitatively, they behaved similarly to HDMPP: with increasing amphiphile content in the EPC bilayer the percentage of lipid contributing to the ^1H NMR high-resolution spectrum increased. However, there were quantitative differences between the effect of various amphiphiles. Depending on the chain length of the alkyl or acyl group R_1 and on the nature of the R_2 substituent bound to the phosphate group, the detergent was more or less efficient at inducing vesiculation.

The detergent-like action of charged lysophospholipids is shown in Figure 3B. It can be seen that mixed lipid dispersions consisting of EPC and lyso-PG behaved similarly to the EPC–amphiphile mixture shown in Figure 3A. With increasing lysophospholipid content, a ^1H high-resolution spectrum developed, the ^1H signal intensity of which increased

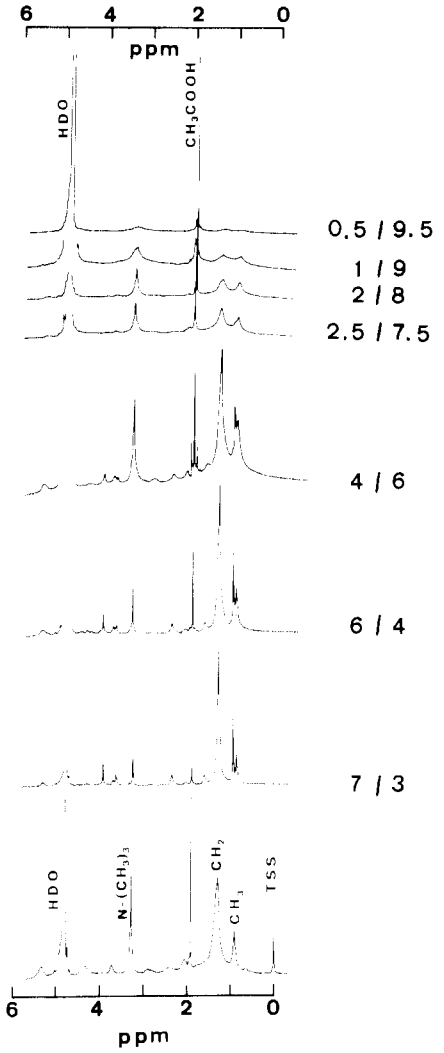

FIGURE 2: 360-MHz ^1H NMR spectra of unsonicated dispersions in ^2H_2O (approximate pH 7–8) consisting of mixtures of HDMPP and EPC. The total lipid concentration (=sum of HDMPP and EPC) was 10 mg/mL. On the right of each spectrum, the weight ratio HDMPP/EPC is given; this was from top to bottom 0.5:9.5 (mole ratio 0.09), 1:9 (0.19), 2:8 (0.42), 2.5:7.5 (0.56), 4:6 (1.13), 6:4 (2.53), and 7:3 (3.9); the bottom spectrum is the ^1H NMR spectrum of a sonicated EPC dispersion (10 mg/mL = 0.013 M) in ^2H_2O (approximate pH ~7). Sonication was carried out as described before (Brunner et al., 1978). The prominent signals from the CH_3, $(CH_2)_n$, and $-N(CH_3)_3$ groups are labeled. For all spectra shown, signal intensities were determined and normalized against an internal CH_3COONa standard (1.35 mg/mL = 16.5 mM). TSS is sodium 3-(trimethylsilyl)propanesulfonate used as an internal shift standard.

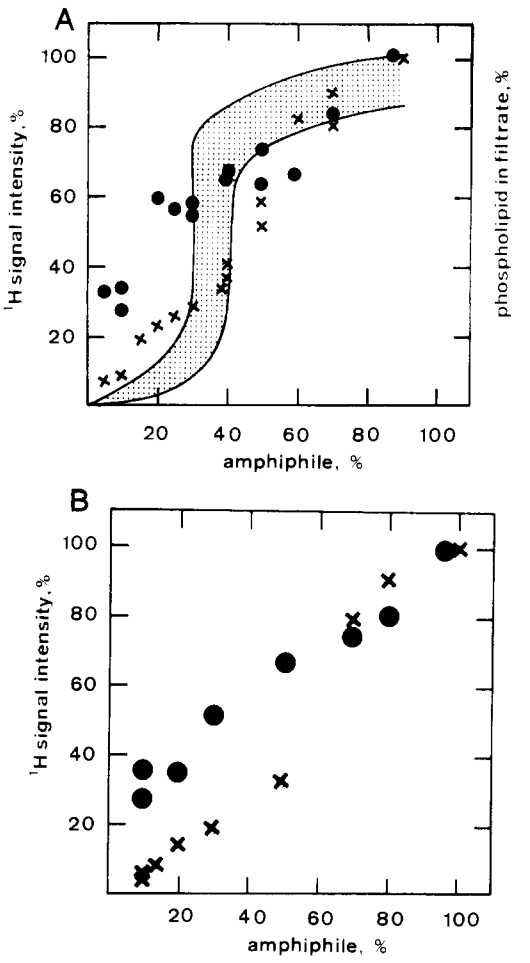

FIGURE 3: (A) ^1H NMR signal intensities as a function of the content of the sodium salt of 2,2-dimethyl-3-hexadecanoylpropanediol 1-phosphate (HDMPP) in mixed dispersions of egg phosphatidylcholine (EPC) and HDMPP. Signal intensities are expressed as percent of the total lipid (=sum of EPC and HDMPP). Mixed dispersions of EPC containing increasing amounts of HDMPP (total concentration ~10 mg/mL) in ^2H_2O were prepared, ^1H NMR spectra were recorded at 360 MHz, and signal intensities were measured as described under Materials and Methods. The hydrocarbon chains of both EPC and HDMPP contribute to the CH_2 signal (×); (●) signal intensity of the $-N(CH_3)_3$ group of EPC. For comparison, the results of the filtration experiments using nucleopore polycarbonate filters (nominal pore diameter 80 nm) are included. The phospholipid content in the filtrate expressed as percent of the total phospholipid of the mixed dispersion is plotted as a function of the HDMPP content (%). The large experimental scatter observed is represented by the stippled area. (B) ^1H NMR signal intensities of mixed EPC/lyso-PG dispersions in ^2H_2O as a function of the lyso-PG content (%). The concentration of the mixed lipid dispersion was ~10 mg/mL, approximate pH 6–7. Intensity of the CH_2 signal arising from the hydrocarbon chains of both EPC and lyso-PG (×); intensity of the $-N(CH_3)_3$ choline signal from EPC (●).

(Figure 3B). A similar relationship was obtained for lyso-PS/EPC mixed dispersions (data not shown). When mixed lyso-PG/EPC dispersions were filtered through nucleopore membranes (of a nominal pore diameter of 80 nm), the percentage of phospholipid recovered in the filtrate correlated reasonably well with the percentage of lipid contributing to the ^1H high-resolution NMR spectrum (data not shown). It is important to note that in both lipid dispersions (Figure 3) the signal intensity of the choline group of EPC was equal to or exceeded that of the CH_2 groups of the hydrocarbon chain. This is clear-cut evidence that the lipid particle giving rise to the high-resolution NMR spectrum consists of both amphiphile and phospholipid.

The effect of increasing concentrations of positively charged amphiphiles present in EPC bilayers on the CH_2 ^1H signal intensity of such dispersions is shown in Figure 4A. With the exception of cetylpyridinium chloride, up to amphiphile contents of about 30% the fraction of lipid giving rise to a high-resolution spectrum was less than ~15%. At higher amphiphile concentrations, there was a sigmoidal increase in the ^1H signal intensity, which was accompanied by an abrupt drop in the turbidity of the sample (cf. Figure 4A,B). Visually, the lipid dispersion clarified at amphiphile concentrations > 40%. The amphiphile most effective at solubilizing EPC bilayers was cetylpyridinium chloride. Included in Figure 4B is the ESR order parameter S_{33}. For all three tetraalkylammonium compounds investigated, the order parameter S_{33} decreased continuously up to an amphiphile concentration of ~40%, which reflects the perturbation of the EPC bilayer by the presence of the amphiphile. Above about 40% amphiphile and coinciding with the drop in absorbance, there was a dis-

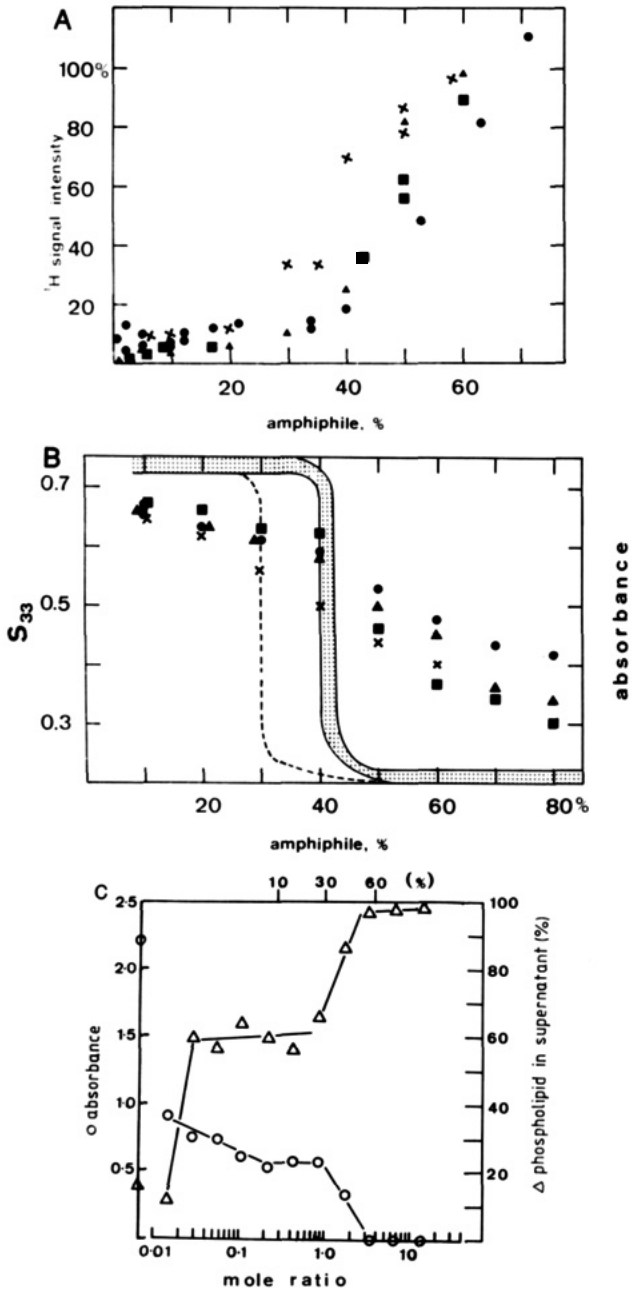

FIGURE 4: (A) Signal intensities of ^{1}H NMR spectra recorded from mixed dispersions of EPC and positively charged amphiphiles as a function of the amphiphile content (%). Mixed lipid dispersions at 10 mg/mL in H_2O (approximate pH 5–6) were prepared from EPC and various positively charged detergents[DTAB (■), TTAB (▲), CTAB (●) and CPC (×)] as described under Materials and Methods. ^{1}H NMR spectra were recorded at 360 MHz, and the intensity of the CH_2 signal was measured and expressed as percent of the total lipid. (B) The ESR order parameter S_{33} of the aqueous mixed lipid dispersions described in (A) as a function of the amphiphile content. The meaning of the symbols is as in (A). The order parameter S_{33} of 5-doxylstearic acid incorporated in the mixed bilayers was determined as described by Hauser et al. (1982). The dashed line represents the turbidity expessed in arbitrary units of mixed EPC/CPC dispersions as measured by the absorbance at 340 nm. The stippled area encloses all the turbidity curves measured for mixed dispersions of EPC containing either DTAB, TTAB, or CTAB. (C) Absorbance [(○) left-hand ordinate] and amount of phospholipid remaining in the supernatant [(△) right-hand ordinate] of a mixed DTAB/EPC dispersion as a function of the DTAB/EPC mole ratio (bottom abscissa); the numbers on the top abscissa are weight percent of DTAB). The mixed lipid dispersions (1 mg EPC/mL) in H_2O were made up as described under Materials and Methods and their turbidity was measured as absorbance at 340 nm. The amount of phospholipid (%) remaining in the supernatant was determined by phosphate analysis after centrifugation of the mixed dispersion at 20000g for 5 min.

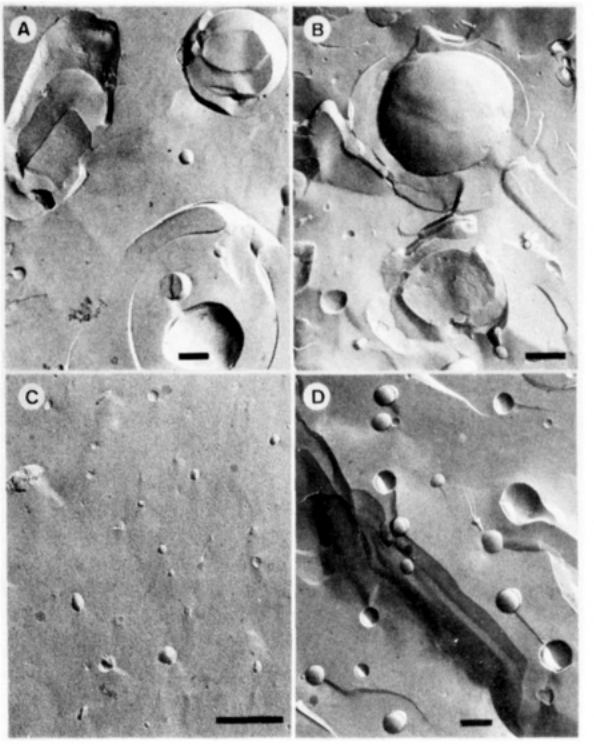

FIGURE 5: Electron micrographs of freeze-fractured samples of mixed dispersions in H_2O of EPC and increasing quantities of CTAB. The mixed dispersions (10 mg/mL) were prepared as described under Materials and Methods. EPC containing 2 wt % CTAB, CTAB/EPC mole ratio 0.04 (A), 10 wt % CTAB, CTAB/EPC mole ratio 0.23 (B), 33 wt % CTAB, CTAB/EPC mole ratio 1 (C), and 20 wt % CPC, CPC/EPC mole ratio 0.55 (D). The bar represents 200 nm.

continuity in S_{33} except for cetylpyridinium, which showed an almost linear decrease in S_{33}. The S_{33} values at high amphiphile content (>80%) are characteristic of small micelles. NMR and ESR evidence taken together indicated therefore that mixed micelles are present in this region of the phase diagram. In Figure 4C the percentage of the EPC remaining in the supernatant after centrifugation at 20000g (△) is shown as a function of the DTAB/EPC mole ratio. The amount of lipid not pelleted under these conditions is compared to the turbidity of the sample (○). The symbols inserted on the y axis represent the values measured for multilamellar EPC dispersions in H_2O. By comparison with these values, it is seen that at mole ratios of 0.01–0.03 the turbidity of the dispersion is less than half of that measured for multilamellar EPC dispersions. At yet higher mole ratios (>1 corresponding to ~35% DTAB, of Figure 4B,C), the turbidity decreased to zero, and concomitantly the phospholipid remaining in the supernatant after centrifugation increased to ~100%. Figure 4C demonstrates that the absorbance (turbidity) curve correlates well with the curve of the amount of phospholipid recovered in the supernatant. Both curves depicted in Figure 4C reflect therefore adequately the physical changes of the lipid dispersions indicated by the ^{1}H NMR signal intensity measurements.

Electron micrographs of freeze-fractured preparations of mixed CTAB/EPC dispersions in H_2O are presented in Figure 5A–C. These mixed dispersions of CTAB/EPC form apparently smectic (lamellar) phases, a conclusion that is supported by ^{31}P NMR (Figure 6). Figure 5A shows that at low CTAB contents of up to ~10% large vesicles are present with a diameter ranging from 0.1 μm to several micrometers. Cross sections of these vesicles reveal smaller vesicles entrapped in the aqueous vesicle cavity. Sometimes, cross sections of large

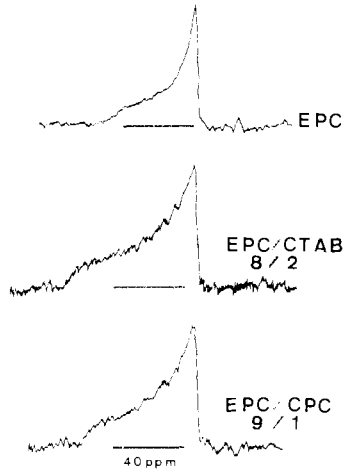

FIGURE 6: Proton-decoupled ^{31}P powder NMR spectra of mixed aqueous dispersions of EPC and positively charged amphiphiles in H_2O. Spectra of EPC (top), CTAB/EPC (wt ratio 0.25, mole ratio 0.52) (middle), and CPC/EPC (wt ratio 0.11, mole ratio 0.25) (bottom) were recorded on a Bruker CXP spectrometer at 121.47 MHz operating in the Fourier-transform mode. The Hahn spin-echo method was used [for details, see Ghosh et al. (1985)].

vesicles show multilamellar stacking reminiscent of PC bilayers in H_2O except that the swelling process seems to have greatly exceeded that of PC bilayers. At concentrations in excess of ~10% CTAB (CTAB/EPC mole ratio = 0.23), such multilamellar structures were no longer observed. At the same time, the vesicle size decreased with increasing amphiphile content (Figure 5C); at 33% CTAB, a large proportion of the total lipid was present as SUV of an average diameter of 25 ± 3 nm (Figure 5C). This is close to that of sonicated EPC dispersions (Hauser et al., 1973). Mixed dispersions of CPC/EPC (20% CPC, mole ratio = 0.55) consisted of unilamellar vesicles ranging in diameter from ~25 to ~250 nm (Figure 5D). With CTAB contents > 33%, the population of SUV increased, and at the same time, the formation of small mixed micelles consisting of CTAB and EPC commenced. This behavior is entirely consistent with the NMR measurements in Figure 4, which show that at these CTAB contents the ^1H signal intensity increased steeply to ~100%. Unfortunately, we were unable to produce visible structures from micelles by freeze-fracture electron microscopy. Mixed dispersions of EPC and other amphiphiles such as DTAB, TTAB, or HDMPP behaved qualitatively similarly to those in Figure 5 when examined by freeze-fracture electron microscopy. Quantitative differences were observed between different amphiphiles regarding the amphiphile content at which SUV and small mixed micelles were formed.

In Figure 6, ^{31}P powder NMR spectra are shown of unsonicated EPC dispersions and mixtures consisting of EPC and CTAB or CPC. The spectral shape is typical for liquid-crystalline phospholipid bilayers and is characteristic of an axially symmetric chemical shielding tensor. It is worth noting that the addition to EPC of 10–20% of a positively charged amphiphile produced a significant increase in the chemical shielding anisotropy $\Delta\sigma$ represented by the two edges of the spectra shown in Figure 6 [cf. Balgavy et al. (1984)].

Spontaneous Vesiculation Induced by Drugs. Many drugs are amphiphilic, surface active molecules with one or more groups that are usually at least partially ionized at neutral pH. Due to these detergent-like properties, they will have a great tendency to orient at lipid–water interfaces, and by doing so, they will impart a net surface charge to neutral lipid bilayers. From the results discussed above, it is likely that a system of lipid and drug that forms a smectic (lamellar) phase in H_2O

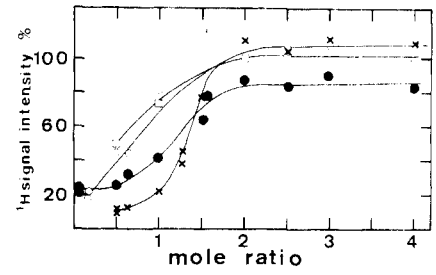

FIGURE 7: Signal intensities of ^1H high-resolution NMR spectra recorded from mixed chlorpromazine/EPC dispersions in ^2H_2O as a function of the chlorpromazine/EPC mole ratio. Mixed dispersions of chlorpromazine and EPC in ^2H_2O were prepared at 10 mg/mL, approximate pH 6–7, as described under Materials and Methods. Signal intensities were measured for the CH_2 signal of the phospholipid hydrocarbon chains (×) and the $-N(CH_3)_3$ choline group (●) and the aromatic (○) and the $-N(CH_3)_2$ protons (□) of chlorpromazine.

behaves similarly to the lipid–detergent systems already discussed. This is borne out by the following experiments. The effect of the drug chlorpromazine on the phase behavior of EPC was followed by measuring ^1H signal intensities as a function of the drug/phospholipid mole ratio (Figure 7). At mole ratios < 1, the signal intensity is less than ~20% of the expected signal intensity. Above a drug/phospholipid mole ratio of ~1, the intensity of the ^1H signals from both lipid and drug increased simultaneously, approaching ~100% at mole ratios > 1.5. The fact that all the protons contributed to the ^1H signal intensity indicates that the lipid structures present under these conditions are particles with a diameter $\lesssim 0.1$ μm. By using $Pr(NO_3)_3$ or $K_3Fe(CN)_6$ as shift reagents in the way as described previously (Bystrov et al., 1971; Hauser & Barratt, 1973; Hauser, 1976; Hutton et al., 1977), it could be shown that the predominant lipid structures present are SUV (data not shown). The observation of spin–spin coupling in the ^1H NMR spectra of dispersions containing excess chlorpromazine (mole ratio > 1.5) indicates that some of the lipid must be present as mixed micelles consisting of EPC and drug. In excess chlorpromazine, the population of mixed micelles grew at the expense of SUV.

The interepretation of the data in Figure 7 is corroborated by freeze-fracture electron microscopy. At drug/phospholipid mole ratios <1, multilamellar liposomes, oligomeric lipid vesicles, i.e., vesicles containing smaller unilamellar vesicles entrapped in their cavity, and LUV were observed. The lipid particles are highly polydisperse, their size ranging from ~0.1 μm to several micrometers (electron micrographs were similar to that of EPC and gramicidin S dihydrochloride shown in Figure 8A). In the compositional range where the ^1H signal intensity increased sharply (Figure 7), the predominant structure was the SUV as confirmed by freeze-fracture electron microscopy (Figure 8C). The speckled background of this electron micrograph may be due to the presence of small mixed micelles with a diameter <10 nm (see arrows, Figure 8C). A number of amphiphilic, surface-active drugs of different chemical structure were investigated as to their effect on EPC bilayers. From this comparative study, it can be concluded that the behavior of chlorpromazine (Figure 7) is representative. Different drugs, however, differed in their efficacy of producing SUV.

As an example of a pharmacologically active peptide, the effect of gramicidin S dihydrochloride on the phase behavior of PC was studied. Gramicidin S dihydrochloride is a surface-active, cyclic decapeptide containing two positively charged ornithins per molecule as well as some hydrophobic amino acids. It can be shown by particle microelectrophoresis that as a surface active peptide it orients at the PC–water

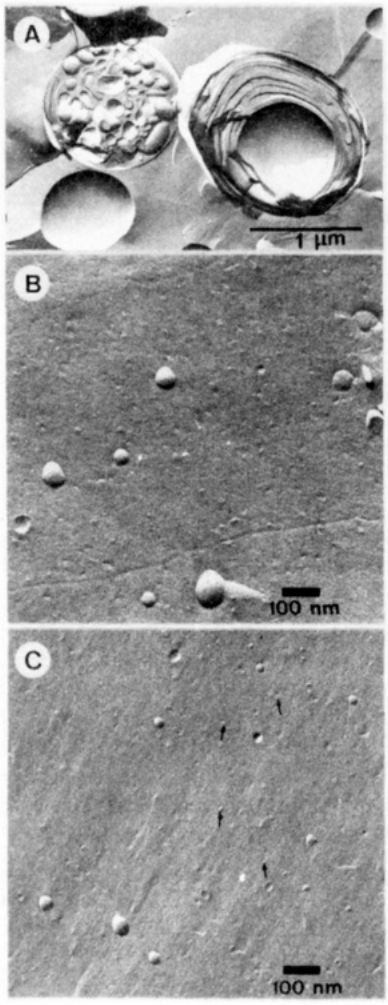

FIGURE 8: Electron micrographs of freeze-fractured preparations of mixed dispersions of EPC and a charged drug in H_2O. EPC and either gramicidin S dihydrochloride or chlorpromazine were mixed in $CHCl_3/CH_3OH$ (2:1 v/v), and the solution was evaporated as described under Materials and Methods. The thoroughly dried mixed film was dispersed by adding the appropriate amounts of H_2O, and if necessary, the pH was adjusted to neutrality with dilute HCl or NaOH. (A) Gramicidin S dihydrochloride/EPC mole ratio 0.02; phospholipid concentration ~10 mg/ml. (B) [EPC] = 10 mg/mL; [gramicidin S dihydrochloride] = 8.8 mg/mL; gramicidin S dihydrochloride/EPC mole ratio = 0.6. (C) [EPC] = 10 mg/mL, [chlorpromazine] = 9.5 mg/mL, chlorpromazine/EPC mole ratio = 2. The arrows probably indicate small, mixed micelles.

interface, imposing a net positive charge on the PC surface (data not shown).

Qualitatively, gramicidin S dihydrochloride can be expected to behave like other surface-active drugs or charged amphiphiles. This is borne out by experiment. Panels A and B of Figure 9 show the ^1H signal intensities of EPC and dimyristoyl-PC, respectively, as a function of the peptide/PC mole ratio. Qualitatively, similar plots were obtained for the two PCs (Figure 9A,B), which were also similar to the corresponding relations obtained with charged amphiphiles (cf. Figures 3A and 4A) or chlorpromazine (cf. Figure 7). The main difference was in the position at which the increase in ^1H signal intensity occurred. The dotted lines represent the transmittance of the dispersions, indicating that the clarification of the dispersion correlates quite well with the increase in ^1H signal intensities. The clarification of the mixed peptide/EPC dispersion is also apparent from Figure 9C, showing turbidity (as absorbance at 340 nm) and the percentage of phospholipid remaining in the supernatant as a function of the peptide/phospholipid mole ratio. We interpret the first de-

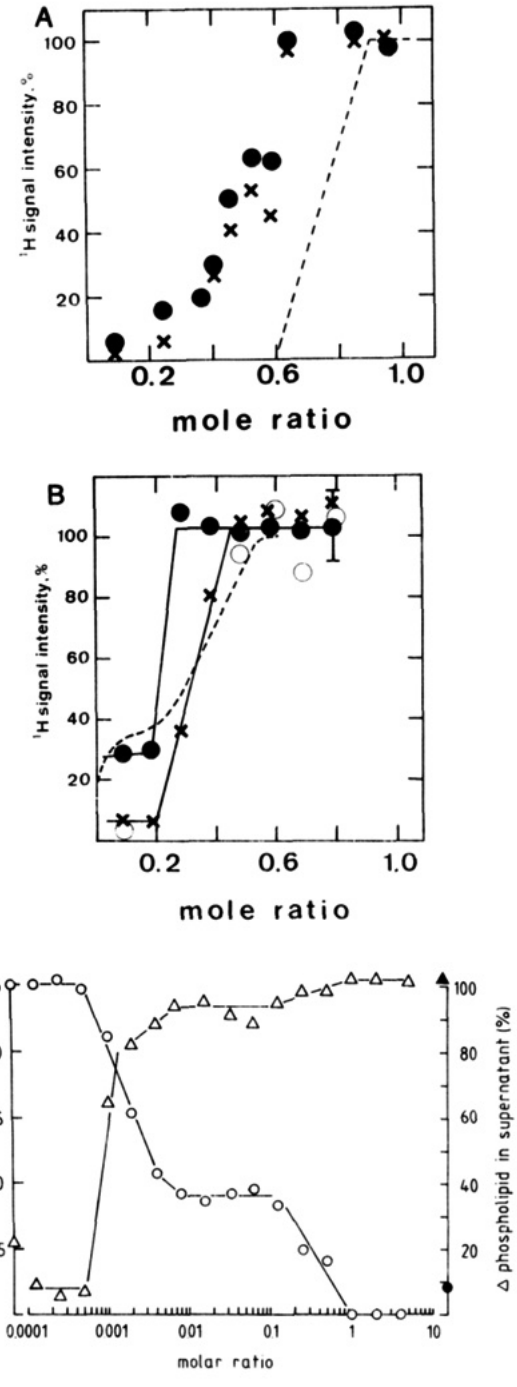

FIGURE 9: (A) Signal intensities of the ^1H high-resolution NMR spectra recorded from mixed gramicidin S dihydrochloride/EPC dispersions as a function of the gramicidin S dihydrochloride/EPC mole ratio. Mixed dispersions in ^2H_2O of EPC (10 mg/mL) containing increasing quantities of gramicidin S dihydrochloride were prepared as described under Materials and Methods. Intensities were measured for the CH_2 signal (×) and the $-N(CH_3)_3$ choline group (●). The dotted line represents the transmittance (%) of the sample. (B) Signal intensities of the ^1H high-resolution NMR spectra recorded from mixed gramicidin S dihydrochloride/dimyristoyl-PC dispersions as a function of the peptide/phospholipid mole ratio. The symbols are as described under (A); aromatic protons (○). The dotted line represents the transmittance (%) of the dispersion. (C) Light scattering [(○) measured as absorbance at 340 nm] of mixed dispersions in H_2O of EPC and gramicidin S dihydrochloride as a function of the gramicidin S dihydrochloride/EPC mole ratio. Included is the amount (%) of phospholipid remaining in the supernatant after centrifugation at 20000*g* for 5 min (△). The open symbols on the left-hand *y* axis represent the values measured for multilamellar EPC dispersions in H_2O; the closed symbols on the right-hand *y* axis represent those measured for sonicated EPC dispersions in H_2O.

crease in absorbance (○) at a mole ratio of $\sim 5 \times 10^{-4}$ M as being due to the disruption of the multilamellar PC liposomes, leading to large oligomeric and unilamellar vesicles. The absorbance is at least halved with respect to that of multilamellar PC vesicles [(○) on the left-hand ordinate]. As the absorbance decreased, the amount of PC remaining in the supernatant after centrifugation increased steeply, indicating that most of the lipid structures are too small to be pelleted under these conditions. As the peptide/phospholipid mole ratio increased above ~0.1, the absorbance decreased further, reaching zero at a mole ratio of ~1. At the same time, the amount of lipid in the supernatant rose to 100%. The value for the absorbance (●) and the amount of lipid present in the supernatant (▲) of a sonicated EPC dispersion are included on the right-hand ordinate for comparison (Figure 9C). The second decrease in absorbance at a mole ratio of ~0.1 and the concomitant increase in the amount of phospholipid in the supernatant are ascribed to the formation of SUV. The fact that the absorbance practically decreased to zero is probably due to a second process leading to the formation of small mixed micelles.

The data for the system gramicidin S dihydrochloride/dimyristoyl-PC were quite similar to those of EPC shown in Figure 9C and were not included for clarity sake. Freeze-fracture electron microscopy supports the interpretation of the data in Figure 9 given above. Mixed EPC dispersions in H_2O containing gramicidin S dihydrochloride up to a mole ratio of ~0.02 are polydisperse, consisting of highly swollen, multilamellar or oligomeric vesicles of a diameter of about 1 μm and LUV; the latter may contain small unilamellar vesicles entrapped in their internal aqueous cavity (Figure 8A). In the region of the steep increase in ^1H signal intensity (Figure 9A,B), the predominant lipid structure present is the SUV (Figure 8B). As the absorbance decreased to zero (at peptide/lipid mole ratios of 0.8, Figure 9C), small mixed micelles were formed as evident from ^1H NMR; these might be responsible for the speckled background of the electron micrograph shown in Figure 8B,C (see arrows).

Discussion

It should be stressed at the outset that the work presented here is on lipids and lipid mixtures forming smectic (lamellar) phases when dispersed in H_2O. Different physical methods were used to characterize the resulting aqueous dispersions. ^1H high-resolution NMR spectroscopy was used routinely to differentiate between small (diameter < 0.1 μm) and large lipid aggregates (diameter > 0.1 μm). It has been shown before (Penkett et al., 1968; Finer et al., 1972; Finer, 1973; Stockton et al., 1976; Bloom et al., 1975; Wennerström & Ulmius, 1976; Hauser & Gains, 1982) that only small phospholipid aggregates such as micelles or SUV of diameter < 0.1 μm contribute to the high-resolution NMR spectrum; the signal intensity was shown to be a good measure of the amount of lipid present in these small aggregates. On the basis of this observation, we propose an operational definition of SUV and LUV: SUV have a diameter smaller than about 0.1 μm, giving rise to a high-resolution NMR spectrum, while LUV have a diameter >0.1 μm, giving a broad-line spectrum. It was further demonstrated that there is a good correlation between the signal intensity of the ^1H high-resolution NMR spectrum and the population of SUV determined by gel filtration on Sepharose 4B (Finer et al., 1972; Hauser & Gains, 1982). From an inspection of Figures 3A, 4, 5, and 9, it is clear that the NMR method is in reasonably good agreement with other methods used here to characterize lipid dispersions in terms of size and size distribution. The agreement between the ^1H signal intensity of the hydrocarbon chain protons and the amount of lipid passing through a nucleopore filter of pore diameter of ~80 nm is satisfactory (Figure 3A). This agreement supports the conclusion that the exclusion limit of lipid particles that do not contribute to the high-resolution NMR spectrum is about 80–100 nm (Finer et al., 1972). There is also good qualitative agreement between the ^1H signal intensity measurement and the population of SUV as determined by freeze-fracture electron microscopy (for instance, compare Figure 4A with 5 and Figures 7 and 9A with 8). while the ^1H NMR signal intensity was used as a measure of the amount of lipid present as small aggregates (diameter < 0.1 μm), other NMR parameters and methods are required to differentiate between SUV and micelles. The lines arising from SUV are too broad to show spin–spin hyperfine interactions, while those of micelles usually do. Furthermore, micelles are readily detected by adding shift reagents of the lanthanide series. In the presence of paramagnetic ions, 100% of the signal intensity originating from the polar group of the micelles is shifted (Hauser et al., 1975). In contrast, when closed unilamellar vesicles interact with impermeable lanthanide ions, only part of the polar group signal is shifted. It has been shown before that the proportion of the signal intensity shifted corresponds to the proportion of molecules present on the outer layer of the bilayer exposed to the paramagnetic lanthanide ion. Hence, the criterion whether or not spin hyperfine interaction is observed and the effect of impermeable shift or broadening reagents can be used to differentiate between SUV and micelles.

As pointed out previously (Hauser, 1984), on the basis of the swelling in H_2O, lipids forming smectic phases may be grouped into two classes: (I) uncharged and isoelectric lipids showing no or limited swelling in H_2O; (II) charged lipids showing continuous swelling with increasing water content. Representative phospholipids of these two classes are phosphatidylcholine and phosphatidylserine, respectively. Further, the thermodynamically most stable structure in excess water of class I lipids has been shown to be the multilamellar liposome whereas that of class II lipids is the unilamellar vesicle. Vesicles thus formed are polydisperse, their size varying between 0.05 μm and several micrometers with a peak unusually between 0.1 and 1 μm. Some of these unilamellar vesicles, particularly large ones, have been described as oligomeric, oligolamellar, or multicompartment vesicles: they contain smaller unilamellar vesicles entrapped in their internal aqueous cavity (Hauser et al., 1983; Hauser, 1984). It should be emphasized that unilamellar vesicles only form when films of charged lipids are dispersed in H_2O or salt solutions of moderate ionic strength ($I < 0.2$); this is, however, not true when solutions of higher ionic strength are used or when polyvalent cations are present (Hauser, 1984; Hauser & Shipley, 1983). Under these conditions, negatively charged phospholipids such as phosphatidylserines behave like phosphatidylcholines: for instance, in 0.5 M NaCl they exhibit limited swelling and form therefore multilamellar liposomes in excess NaCl solutions of this molarity. Furthermore, it was also shown before that continuous swelling and the spontaneous vesiculation are not only properties characteristic of pure charged phospholipids but more importantly also of lipid mixtures of a relatively low surface charge density (Gulik-Krzywicki et al., 1969; Cowley et al., 1978).

The surface charge density of natural and synthetic phosphatidylserines varies between ~23 and 36 $\mu C/cm^2$, depending on the nature of the fatty acyl chains. Continuous swelling behavior was induced in EPC bilayers by doping them with

a few percent of charged amphiphile such as cetyltrimethylammonium bromide or sodium oleate (Gulik-Krzywicki et al., 1969). The surface charge density of these lipid mixtures was about 1–2 μC cm^2, less than one-tenth of that of phosphatidylserines. From their continuous swelling in H_2O, mixed bilayers exceeding this threshold charge density (Gulik-Krzywicki et al., 1969) can be expected to undergo spontaneous vesiculation in excess H_2O. This is borne out by the experiments presented in Figures 2–4. Mixtures consisting of EPC and a charged amphiphile undergo spontaneous vesiculation when H_2O is added to the dried film and a dispersion is made by shaking. Up to amphiphile concentrations at which the ^1H signal intensity rose steeply, the vesiculation led to mainly LUV and oligomeric large vesicles. At higher amphiphile contents, the fraction of lipid present as SUV increased, and in the compositional range where the increase in ^1H NMR signal intensity was observed, SUV were the most stable structure. From a practical point of view, it is important to realize that this behavior is a general one and characteristic of charged amphiphiles with a single hydrocarbon chain of 14 or more C atoms, such as charged detergents or lysophospholipids. We can conclude that in the phase diagram of three-component systems consisting of EPC, a charged, single-chain amphiphile, and water there is a compositional region, though narrow it may be, where the SUV is the thermodynamically most stable structure (Hauser et al., 1985). Rydhag et al. (1982a,b) showed that this is true for the system dimyristoyl-PC, CTAB, and H_2O. From the data presented here, the mechanism by which increasing quantities of a charged amphiphile result in the formation of SUV is not clear. Preliminary results suggest that a prerequisite for this is the asymmetric transverse distribution of the charged amphiphile. The mechanism of the spontaneous vesiculation with the formation of SUV will be the subject of a separate publication.

The behavior of single-chain amphiphiles is contrasted by negatively charged diacyl phospholipids bearing a net negative charge at neutral pH such as phosphatidylserine or phosphatidic acid. Spontaneous vesiculation of these lipids, either in pure form or as mixtures with neutral (isoelectric) lipids, leads to LUV with a diameter usually greater than 0.1 μm. SUV are not produced under these circumstances. In this context, the method of spontaneous vesiculation based on a transient pH change is worth mentioning because it fits the general pattern emerging. Phosphatidic acid and mixtures of it with EPC and other neutral lipids have been shown to undergo spontaneous vesiculation if the pH is raised transiently to pH 10–12, ensuring complete ionization of the phosphatidic acid molecule (Hauser & Gains, 1982; Hauser et al., 1983; Gains & Hauser, 1983). The resulting vesicles are usually a mixture of SUV and LUV, depending on the amount of phosphatidic acid present. In this case, a diacyl phospholipid undergoes spontaneous vesiculation with the formation of SUV. This is not inconsistent with the general rule discussed above because diacylphosphatidic acid in aqueous dispersions at a pH >10 is fully ionized, containing two charges per two hydrocarbon chains; hence, it attains detergent-like properties and behaves in a way similarly to a single-chain amphiphile (detergent).

Many pharmacologically active compounds are amphiphilic and surface-active; as such, they orient at neutral lipid–water interfaces imparting a net surface charge to the neutral lipid surface. We have tested a number of amphiphilic drugs as to their effect on the phase behavior of EPC and can conclude that the behavior of chlorpromazine depicted in Figure 7 is representative. Provided the surface charge density generated by the surface-bound drug exceeds the threshold value discussed above, the system EPC, drug, and H_2O undergoes spontaneous vesiculation. The nature of the vesicles formed depends on the drug/phospholipid mole ratio. Both chlorpromazine and the surface active peptide gramicidin S dihydrochloride have a detergent-like, solubilizing effect on PC bilayers. The lytic properties of gramicidin S dihydrochloride were described before (Finer et al., 1969). As with the three-component system EPC–detergent–H_2O, there is a, though narrow, compositional range in the phase diagram EPC–chlorpromazine–H_2O or PC–gramicidin S dihydrochloride–H_2O where the SUV is the thermodynamically most stable structure. Furthermore, it is clear that by decreasing the detergent/phospholipid or drug/phospholipid mole ratio the size of the resulting unilamellar vesicles can be increased.

The phase behavior of the system lipid-charged drug–H_2O discussed here may have important implications in terms of drug encapsulation and delivery. The very presence of the drug in the lipid bilayer can be utilized to induce spontaneous vesiculation and to produce the vehicle proper for the delivery of the drug. In contrast to the standard methods commonly used to produce unilamellar vesicles, the method of spontaneous vesiculation described here is simple and quick. Upon the addition of H_2O or aqueous solvents of moderate ionic strength to a lipid film (smetic phase) dried down on the glass wall of a round-bottom flask, unilamellar vesicles form spontaneously. All that is required is the surface charge density of the lipid bilayer to exceed a certain threshold value. Spontaneous vesiculation occurs over a wide range of amphiphile/lipid composition with the average vesicle size depending on the amphiphile/lipid mole ratio: with increasing amphiphile content, the average vesicle size decreases consistent with results reported previously (Schurtenberger & Hauser, 1984). As shown in Figures 3, 4, 7, and 9, the formation of SUV is restricted to a rather narrow range of amphiphile/lipid mole ratios, which has to be determined experimentally. The method of spontaneous vesiculation has the advantage that it does not require any elaborate laboratory equipment and it does not involve tedious procedures such as sonication, dialysis, or gel filtration.

Registry No. HDMPP, 90825-46-0; CTAB, 57-09-0; TTAB, 1119-97-7; DTAB, 1119-94-4; CPC, 123-03-5; chlorpromazine, 50-53-3; gramicidin S, 113-73-5.

References

Balgavy, P., Gawrisch, K., & Frischleder, H. (1984) *Biochim. Biophys. Acta 772*, 58–64.

Bloom, M., Burnell, E. E., Valic, M. I., & Weeks, G. (1975) *Chem. Phys. Lipids 14*, 107–112.

Brunner, J., Hauser, H., & Semenza, G. (1978) *J. Biol. Chem. 253*, 7538–7546.

Bystrov, V. F., Dubrovina, N. I., Barsukov, L. I., & Bergelsen, L. D. (1971) *Chem. Phys. Lipids 6*, 343–350.

Cowley, A. C., Fuller, N. L., Rand, R. P., & Parsegian, V. A. (1978) *Biochemistry 17*, 3163–3168.

Eibl, H. (1980) *Chem. Phys. Lipids 26*, 405–429.

Finer, E. G. (1973) *J. Magn. Reson. 13*, 76–86.

Finer, E. G., Hauser, H., & Chapman, D. (1969) *Chem. Phys. Lipids 3*, 386–392.

Finer, E. G., Flook, A. G., & Hauser, H. (1972) *Biochim. Biophys. Acta 260*, 49–69.

Gains, N., & Hauser, H. (1983) *Biochim. Biophys. Acta 731*, 31–39.

Gains, N., & Hauser, H. (1984) in *Liposome Technology* (Gregoriadis, G., Ed.) Vol. I, pp 67–78, CRC Press, Boca Raton, FL.

Gains, N., & Hauser, H. (1985) *J. Membr. Sci. 22*, 225-234.
Ghosh, R., Bachofen, R., & Hauser, H. (1985) *Biochemistry 24*, 983-989.
Gulik-Krzywicki, T., Tardieu, A., & Luzzati, V. (1969) *Mol. Cryst. Liq. Cryst. 8*, 285-291.
Hauser, H. (1976) *J. Colloid Interface Sci. 55*, 85-93.
Hauser, H. (1984) *Biochim. Biophys. Acta 772*, 37-50.
Hauser, H., & Barratt, M. D. (1973) *Biochem. Biophys. Res. Commun. 53*, 399-405.
Hauser, H., & Gains, N. (1982) *Proc. Natl. Acad. Sci. U.S.A. 79*, 1683-1687.
Hauser, H., Oldani, D., & Phillips, M. C. (1973) *Biochemistry 12*, 4507-4517.
Hauser, H., Phillips, M. C., Levine, B. A., & Williams, R. J. P. (1975) *Eur. J. Biochem. 58*, 133-144.
Hauser, H., Gains, N., Semenza, G., & Spiess, M. (1982) *Biochemistry 21*, 5621-5628.
Hauser, H., Gains, N., & Müller, M. (1983) *Biochemistry 22*, 4775-4781.
Hauser, H., Gains, N., & Lasic, D. D. (1985) in *Proceedings S.I.F.* (Degiorgio, V., & Corti, M., Eds.) Course XC, p 648, North-Holland, Amsterdam.
Hutton, W. C., Yeagle, P. L., & Martin, R. B. (1977) *Chem. Phys. Lipids 19*, 255-265.
Müller, M., Meister, N., & Moor, H. (1980) *Mikroskopie 36*, 129-140.
Penkett, S. A., Flook, A. G., & Chapman, D. (1968) *Chem. Phys. Lipids 2*, 273-290.
Rydhag, L., & Gabran, T. (1982) *Chem. Phys. Lipids 30*, 309-324.
Rydhag, L., Steinus, P., & Oedberg, L. (1982) *J. Colloid Interface Sci. 86*, 274-276.
Schurtenberger, P., & Hauser, H. (1984) *Biochim. Biophys. Acta 778*, 470-480.
Stockton, G. W., Polnaszek, C. F., Tulloch, A. P., Hasan, F., & Smith, I. C. P. (1976) *Biochemistry 15*, 954-966.
Wennerström, H., & Ulmius, J. (1976) *J. Magn. Reson. 23*, 431-435.

Interaction of Intestinal Brush Border Membrane Vesicles with Small Unilamellar Phospholipid Vesicles. Exchange of Lipids between Membranes Is Mediated by Collisional Contact†

Beat Mütsch, Nigel Gains,‡ and Helmut Hauser*

Laboratorium für Biochemie, Eidgenössische Technische Hochschule, ETH-Zentrum, CH 8092 Zürich, Switzerland

Received September 11, 1985

ABSTRACT: The kinetics of lipid transfer from small unilamellar vesicles as the donor to brush border vesicles as the acceptor have been investigated by following the transfer of radiolabeled or spin-labeled lipid molecules in the absence of exchange protein. The labeled lipid molecules studied were various radiolabeled and spin-labeled phophatidylcholines, radiolabeled cholesteryl oleate, and a spin-labeled cholestane. At a given temperature and brush border vesicle concentration similar pseudo-first-order rate constants (half-lifetimes) were observed for different lipid labels used. The lipid transfer is shown to be an exchange reaction leading to an equal distribution of label in donor and acceptor vesicles at equilibrium (time $t \rightarrow \infty$). The lipid exchange is a second-order reaction with rate constants being directly proportional to the brush border vesicle concentration. The results are only consistent with a collision-induced exchange of lipid molecules between small unilamellar phospholipid vesicles and brush border vesicles. Other mechanisms such as collision-induced fusion or diffusion of lipid monomers through the aqueous phase are negligible at least under our experimental conditions.

Very little is known about how the digested lipids in the lumen of small intestine are absorbed by the enterocytes and pass from there into the lymph system. If only the first step in this process, that is, the interaction of the digested lipid with the absorptive surface of the enterocyte, is considered, then there are two questions. The first concerns the form in which the dispersed and digested lipids are absorbed: it could be monomeric, micellar, and vesicular (Carey et al., 1983). Although for lipids with a relatively high water solubility (or critical micellar concentration) uptake of monomers could be efficient, it would seem that for lipids with a low water solubility (e.g., diacyl phospholipids) uptake is only likely to be efficient if they are dispersed in micelles or bilayer vesicles. The second problem is that the site of lipid absorption on the enterocyte membrane is not known. If only the brush border is considered, then absorption could occur over the total microvillar membrane or be locally restricted.

Here we present part of a systematic study of lipid uptake by the enterocyte. We first chose to investigate lipid transfer between brush border membrane and small unilamellar vesicles made of phosphatidylcholine. The results presented are not only relevant to the question of lipid uptake by the enterocyte

† This work was supported by Swiss National Science Foundation Grant 3.511-0.83 and by the Zentenarfond (ETH-Zuerich). Some of the ESR experiments were carried out by I. Criscuoli in the course of her ETH-Diplomarbeit.

‡ Present address: F. Hoffmann-La Roche & Co., CH 4002 Basel, Switzerland.

0006-2960/86/0425-2134$01.50/0